ELSEVIER

Ceramics International 29 (2003) 183–188

CERAMICS INTERNATIONAL

www.elsevier.com/locate/ceramint

The effect of mullite on the mechanical properties and thermal shock behaviour of alumina–mullite refractory materials

Cemail Aksel*

Department of Materials Science and Engineering, Anadolu University, Iki Eylül Campus, 26555 Eskisehir, Turkey

Received 26 February 2002; received in revised form 4 April 2002; accepted 25 May 2002

Abstract

Mechanical properties and thermal shock behaviour of slip-cast alumina-mullite refractories have been investigated. There was a marked improvement in strength, Young's modulus and fracture toughness values with the addition of finest (~5 μm) mullite particles. The shorter length needle-like mullite particles led to some pull-out and crack deflection. More fracture surface energy was therefore required to connect the cracks for propagation, resulting in a high value of fracture toughness. The resistance to fracture initiation and propagation caused by the thermal stresses was increased, as supported by the R and R_{st} parameters. Therefore, the retained strength was improved by increasing the quench temperature, showing a high resistance to thermal shock.

Keywords: C. Mechanical properties; D. Alumina; D. Mullite; E. Refractory; Thermal shock

1. Introduction

Mullite ($3Al_2O_3{\cdot}2SiO_2$) is a characteristic constituent of all ceramic products made from aluminosilicates, and has recently become a candidate as a high-temperature structural ceramic [1–4], because of its excellent physical properties, such as low dielectric constant, low thermal expansion, high melting point, high resistance to creep, high temperature mechanical stability and thus high thermal shock resistance, and chemical corrosion [5]. Sintering behaviour of mullite-containing powders has been studied over a range of chemical compositions (Al_2O_3/SiO_2 ratio). It has been reported that [5] the observed lattice parameters of mullite samples are significantly influenced by minor compositional changes and different thermal conditions such as temperature of synthesis and both heating and cooling rate. The change in lattice parameters might be due to the disorder between Al and Si ions at high temperatures. Densification measurements have been made for both liquid phase-containing and solid state systems. Small amounts of liquid phase have been observed to have a significant effect on densification rate [6]. Porosity leads to low mechanical strength, but on the other hand, to better thermal shock resistance. For this reason, pull-out, crack branching and deflection mechanisms in alumina–mullite (AM) refractory materials require a weak interface between the additives and matrix, in which needle-like mullite whiskers interlocks alumina grains. Therefore, strong chemical bonding is undesirable if high toughness is required [7]. This structure is apparently responsible for the relatively high strength to be retained mechanical integrity and excellent thermal-shock resistance exhibited by AM refractory materials [8].

Hasselman [9] defined a number of parameters that can be used to predict the thermal shock behaviour of a material. The most widely used of these are the R, and R_{st}. R predicts the maximum allowable temperature difference in a body under conditions of steady heat flow and is expressed as the difficulty of crack initiation [9]. R is given by the formula:

$$\{R = [\sigma{\cdot}(1-\upsilon)]/(E{\cdot}\alpha)\} \quad (1)$$

where σ is strength, E is Young's modulus, ν is Poisson's ratio and α is the mean thermal expansion coefficient of a refractory. α Values, which depend on the Young's modulus, volume fraction and coefficient of thermal

* Tel. +90-222-3350580-81x6355; fax. +90-222-3239501.
E-mail address: caksel@anadolu.edu.tr (C. Aksel).

0272-8842/03/$22.00
PII: S0272-8842(02)00103-7

expansion of each component, can be calculated from the equation derived by Turner [10]. R_{st} parameter [9] can also be used to foresee crack stability and further weakening of a refractory material with increasing severity of thermal shock. R_{st} is given by the following formula:

$$R_{st} = \left[\gamma_i/\left(\alpha^2 \cdot E\right)\right]^{1/2} \quad (2)$$

where γ_i is surface fracture energy. In both cases a high value indicates good resistance to thermal stresses.

It has been reported that [11] it was found to be difficult to improve the fracture toughness of alumina ceramics by the addition of mullite whiskers, as minimal crack deflection by the whiskers and pull-out of the whiskers occurred, and because of the decrease in the Young's modulus; however, further studies are required. For this reason, this present work was carried out. This paper gives information about the relationships between the microstructural characterisation and mechanical properties with the explanation of the reasons for the improvement on mechanical properties and thermal shock behaviour of slip-cast AM refractory materials by the addition of micron size mullite particles.

2. Experimental procedure

Two types of batches were prepared: (i) one containing coarse (−3+1 mm) and medium (−1000+20 μm) alumina-mullite particles, including ~5 μm fine mullite particles (A), and (ii) the other containing only coarse and medium particles, whilst keeping the alumina:mullite ratio constant, without using ~5 μm fine mullite particles (B). Slips were then taken and cast into bars 150×10×15 mm, dried at 110 °C and fired at 1600 °C for ~3 h. Bulk density and apparent porosity were measured using the standard water immersion method [12]. Mechanical and thermal shock testing by water quenching five bars from 1200, 900, 600 and 300 °C to room temperature were carried out. Those bars were tested using a Mayes, SMT50 tensile testing machine in three-point configuration with a support roller span of 110 mm, at a crosshead speed of 1 mm min^{-1}. Strength, σ [13], and Young's Modulus, E [14], values were determined using the standard equations, and five specimens were normally tested to obtain a mean value for each quench temperature:

$$\sigma = \frac{3}{2} \cdot \frac{PL}{WD^2} \quad (3)$$

$$E = L^3 m/\left(4WD^3\right) \quad (4)$$

where P is the load at fracture, L is the length of support span, W is the specimen width, D is the specimen thickness, and m is the slope of the tangent of the initial straight-line portion of the load-deflection curve. The R and R_{st} parameters were also calculated to envisage the resistance to fracture initiation by the thermal stresses and further weakening of a refractory material with increasing severity of thermal shock. Fracture toughness was then measured [15,16] using the single edge notched beam (SENB) technique, with a (6 mm deep) notch cut with a 1 mm thick diamond blade producing a notch to depth ratio of 0.25. Fracture toughness (K_{1c}) was calculated from the maximum load using Eq. (5):

$$K_{1c} = \frac{3PLc^{1/2}}{2WD^2} \quad Y = (2E\gamma_i)^{1/2} = \left(\sigma Y C^{1/2}\right) \quad (5, 6, 7)$$

where c is the notch depth, C is the critical crack length, and Y is a dimensionless number, which is dependent on the geometry of the loading and the crack configuration:

$$Y = \left[A_0 + A_1(c/D) + A_2(c/D)^2 + A_3(c/D)^3 + A_4(c/D)^4\right] \quad (8)$$

with $L/D \approx 8$, $A_0 = +1.96$, $A_1 = -2.75$, $A_2 = +13.66$, $A_3 = -23.98$, $A_4 = +25.22$ [16]. Secondary and back scatter electron images were then made to examine microstructure and fracture surfaces using a CamScan 4 scanning electron microscope.

3. Results and discussion

The density and apparent porosity values of samples were 2.7 g cm^{-3} and 23% for A, and 2.6 g cm^{-3} and 25% for B, respectively. Chemical compositions of these samples were given as follows: 91.4% Al_2O_3, 8.6% SiO_2 (A); and 86.1% Al_2O_3, 13.9% SiO_2 (B). A general microstructure of AM refractory materials with a map distribution of each element has been given in Fig. 1a and b, showing distribution of pores and formation of a crack (Fig. 1a). Thermal expansion mismatch led to large tensile hoop stresses and crack development between alumina and mullite grains, during cooling from fabrication temperature of ~1600 °C, because of the significant difference on the coefficients of thermal expansion, which are ~5.1 MK^{-1} for mullite and ~8.2 MK^{-1} for alumina [17,18]. Microcracks have been observed within both the alumina and needle-like mullite grains, where when the crack reached the needle-like coarse mullite grains, crack propagation decreased steadily (Fig. 1a). On the contrary, when there was no coarse mullite grain between the two coarse alumina grains, cracks propagated rapidly (Fig. 2). The pores, resulting in a weak interface, in these refractory materials, are mainly located close to the interface between the coarsest alumina and mullite grains (Figs. 1a and 2). This indicates that when cracks propagate between the coarse grains and come across to the pores, crack

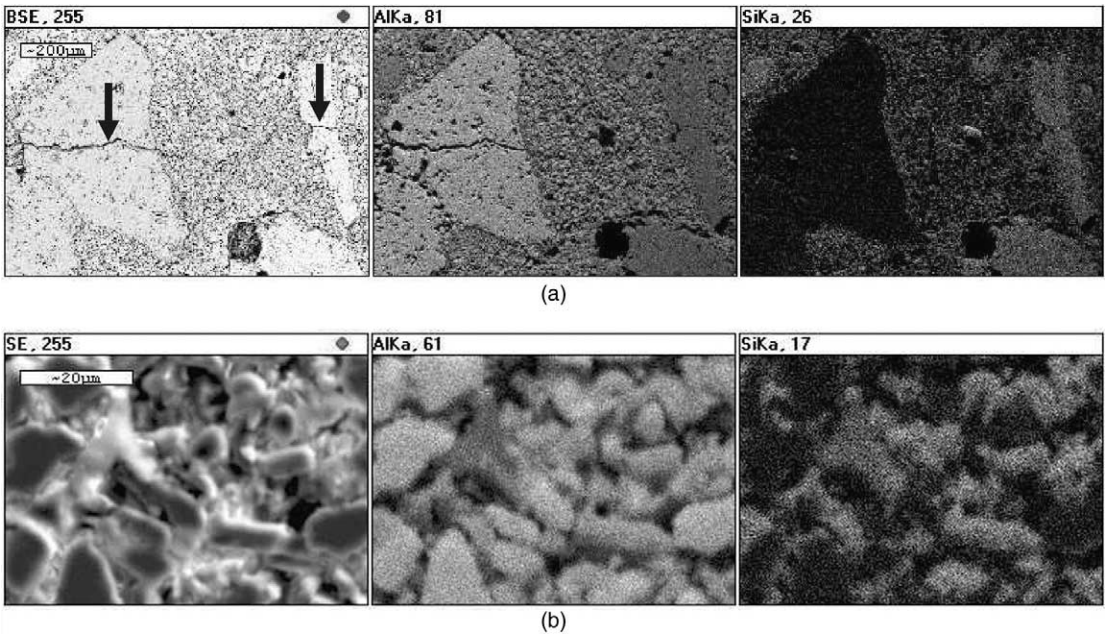

Fig. 1. Map distribution of sample A.

blunting occurs, and thus the resistance to further crack extension increases because of crack deflection and branching mechanisms.

Mechanical properties of samples A and B have been given in Table 1. There was an ~30% increase in the strength of sample A in comparison to sample B. The addition of fine mullite particles provided an improvement in strength, though to a lesser degree, through a reduction in porosity and by faster sintering and hence improved bonding of the matrix. There was also similar improvement observed in the elastic modulus of sample A, indicating that slow crack propagation occurred between the alumina and mullite grains. The calculated critical crack size (C) of sample A was 20% higher than that of sample B. Fracture surface energy (γ_i) of sample A confirmed that ~50% more energy was required to initiate the cracks for propagation compared to B. The R parameter values showed that the difficulty of crack initiation caused by the thermal stresses under conditions of steady heat flow in sample A was >15% higher than that of sample B (Table 1). Furthermore, R_{st} parameter, indicating the maximum allowable temperature difference required to propagate long cracks under severe thermal stress conditions, supported that it would be approximately 40% improvement in the crack stability and further weakening of sample A, with increasing quench temperature, with regard to sample B (Table 1). It would be expected on the basis of the R and R_{st} parameters to show a high resistance to fracture initiation and propagation caused by the thermal stresses as a result of the presence of fine mullite particles. It appears that the amount of cracking and crack size in sample A were limited, and pre-existing cracks could not propagate easily, which is associated with ~40% improvement in fracture toughness of material.

After thermal shock parameters R and R_{st} were calculated, the behaviour of materials was predicted on that basis. These predictions were compared with the experimental thermal shock test data. Thermal shock tests showed that there was a significant rise in the strength of sample A, compared to that of sample B, with increasing quench temperature (Fig. 3a). Fraction of initial strength values (e.g. the portion of retained strength), which are the strengths of bars after quenching relative to initial strengths, were then determined as a function of quench temperature in order to provide a direct indication of resistance to further damage caused by thermal shock. Fraction of initial strength values defined as relative strength have also confirmed that there was an ~50% loss in strength of sample A, but

Table 1
Mechanical properties of samples A and B

Samples	σ (MPa)	E (GPa)	K_{1c} (MPa m$^{1/2}$)	γ_i (J m^{-2})	C (mm)	R (K)	R_{st} (m$^{1/2}$ K$^{1/2}$)
A	10.0±0.7	9.7±1.2	0.7±0.1	25±0.1	1.2±0.2	115±9	1.1±0.1
B	7.8±0.6	7.4±1.1	0.5±0.1	18±0.1	1.0±0.1	99±13	0.8±0.1

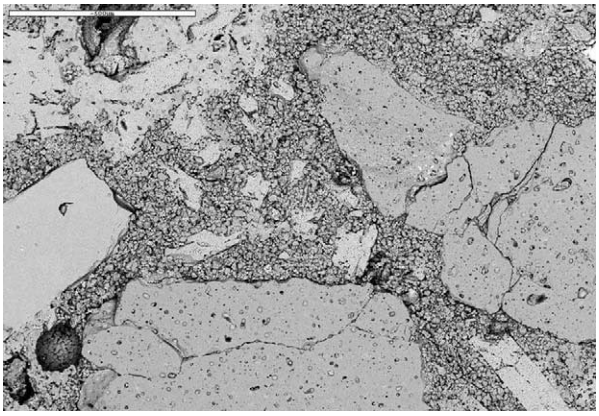

Fig. 2. Microstructure of sample B (scale bar: 500 μm).

~65% loss in strength of sample B, at the maximum quench temperature used (Fig. 3b). Elastic modulus values showed a decreasing trend with increasing quench temperature (Fig. 3c). When the number of cracks and crack lengths increase, the actual area supporting the applied force decreases. Hence an increase in stress for a given load may produce more microcracks. The greater the extent of cracking, the greater the decrease in Young's modulus. On the contrary, modulus of sample A had still slightly higher value than that of B (Fig. 3c). This improvement in strength and Young's modulus values indicates a limited crack size and slow crack propagation as a result of the addition of finest mullite particles. Therefore, the thermal shock resistance of sample A was better than that of B provided adequate strength was retained in the piece.

Crack initiation resistance gives information about the ability of materials to withstand thermal shock, as defined by experience of a rapid temperature change without the initiation of a crack. The assessment of thermal shock damage can be achieved using strength and Young's modulus values. The predictions made from the R and R_{st} parameters were tested by measurements made on thermally shocked refractory materials. The calculated R and R_{st} parameters for those refractory materials showed a good correlation with the retained strength (i.e. strength loss values) after thermal shock testing. It has been confirmed that thermal stress resistance parameters, R and R_{st}, can be used to characterise thermal shock damage of those refractory materials for an industrial applications.

Fracture examination of sample B quenched from 1200 °C showed entirely intergranular fracture in the microstructure (Fig. 4a). Fig. 4b showed that mainly intergranular, but some transgranular cracks occurred through the alumina grains in sample A, where mullite particles were located both at the grain boundaries and within the alumina grains. There was no significant

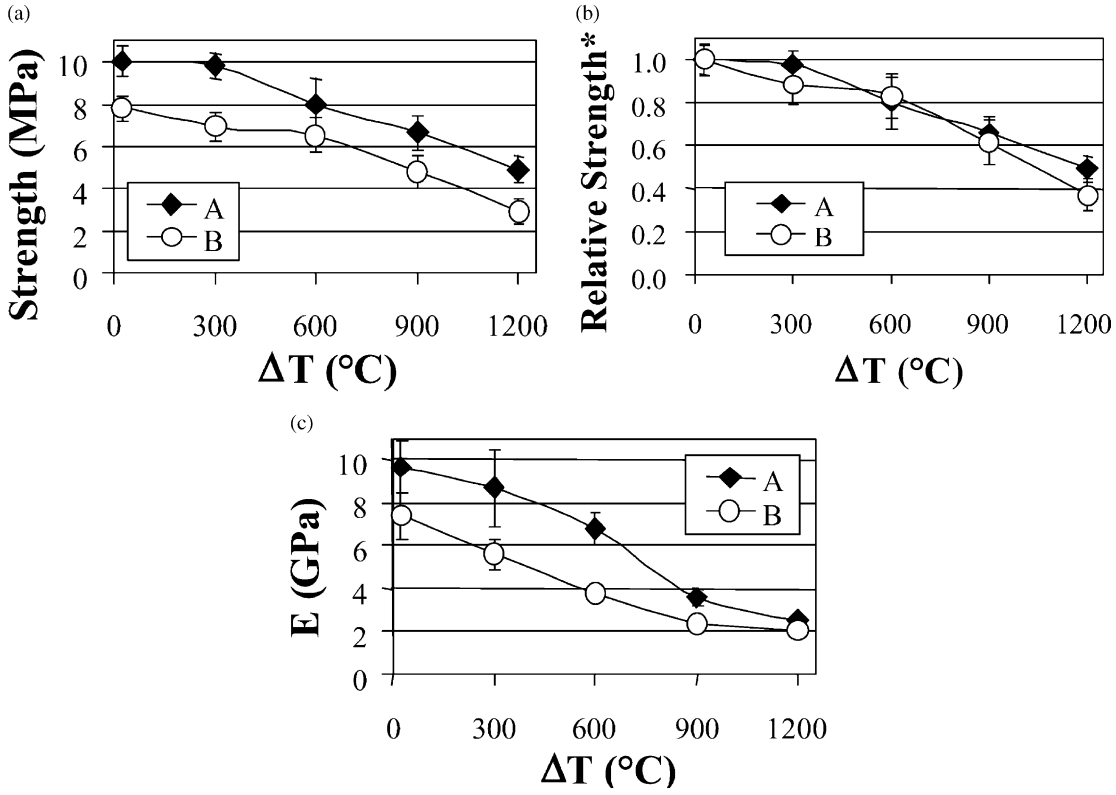

Fig. 3. Mechanical properties as a function of quench temperature: (a) strength, (b) fraction of initial strength*, (c) Young's modulus.

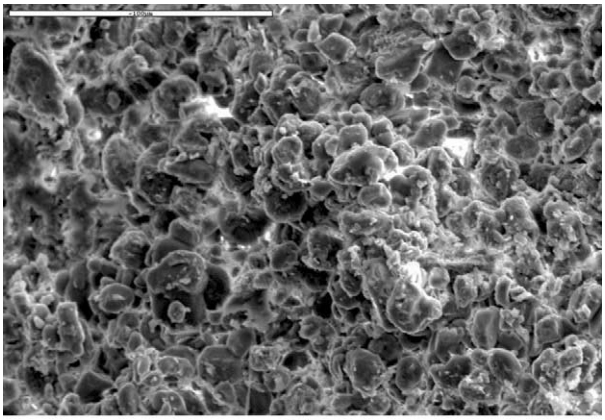

(a)

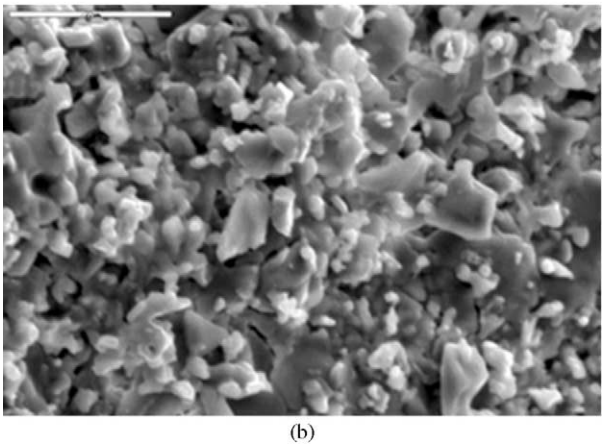

(b)

Fig. 4. Fracture surface of samples, quenched from 1200 °C: (a) sample B (scale bar: 100 μm), (b) sample A (scale bar: 20 μm).

agglomeration of mullite particles associated with non-uniform dispersion that prevents the formation of large microstructural defects. Shorter length, needle-like mullite particles have been observed in the microstructure of sample A (Fig. 1b), which led to some pull-out (Fig. 4b) and crack deflection because of a weak interface between the mullite particles and alumina matrix, associated with the high values of fracture surface energy and fracture toughness. It is also noted that strong chemical bonding is undesirable if high toughness is required, for the applications where high thermal shock resistance is essential. The needle-like fine-grained particles in the microstructure of a material, leading to some pull-out, and interlocking the grains, are apparently responsible for the relatively high strength and fracture toughness, and thus a high thermal-shock resistance exhibited by a slip-cast alumina–mullite refractory.

4. Conclusions

The addition of fine needle-like mullite particles into the slip-cast alumina–mullite refractory materials significantly improved both mechanical and thermal shock properties. Values of strength and elastic modulus increased by about 30%. Fracture behaviour showed a change from mainly intergranular to some transgranular fracture. The amount of energy required to propagate cracks therefore increased by a factor of 1.5, which is associated with a high value of fracture toughness. Pull-out, due to the weak interface, and crack deflection, due to the effect of porosity in the microstructure, both occurred. An improvement in the retained strength with increasing quench temperature indicated that the addition of ~5 μm mullite increased the resistance to crack propagation.

Acknowledgements

The author wishes to thank Professor F.L. Riley and Mr. F. Konieczny for their helpful discussions, and their invaluable expertise in this field was greatly appreciated.

References

[1] T. Takei, Y. Kameshima, A. Yasumori, K. Okada, Crystallisation kinetics of mullite in alumina–silica glass fibers, J. Am. Ceram. Soc. 82 (10) (1999) 2876–2880.
[2] B.B. Ghate, D.P.H. Hasselman, R.M. Spriggs, Synthesis and characterisation of high purity, fine grained mullite, Am. Ceram. Soc. Bull. 52 (9) (1973) 670–672.
[3] D.M. Ibrahim, S.M. Naga, Z.A. Kader, E.A. Salam, Cordierite–mullite refractories, Ceram. Int. 21 (1995) 265–269.
[4] X.C. Zhong, G.C. Sun, Thermomechanical properties of corundum–mullite–zirconia materials, in: UNITECR '97, Proc. Unified Int. Tech. Conf. on Refractories, 5th Biennial Worldwide Congress, Refractories—A Worldwide Technology, New Orleans, 1997, pp. 943–952.
[5] T. Sato, M. Shizuka, M. Shimada, Sintering and characterisation of mullite alumina composites, Ceram. Int. 12 (2) (1986) 61–65.
[6] M.D. Sacks, J.A. Pask, Sintering of mullite-containing materials: 1, effect of composition, J. Am. Ceram. Soc. 65 (2) (1982) 65–70.
[7] J. Wang, M.R. Piramoon, C.B. Ponton, P.M. Marcus, A study in short alumina-fiber-reinforced mullite composites, Trans. J. Br. Ceram. Soc. 90 (4) (1991) 105–110.
[8] K.S. Mazdiyasni, L.M. Brown, Synthesis and mechanical properties of stoichiometric aluminium silicate (mullite), J. Am. Ceram. Soc. 55 (11) (1972) 548–552.
[9] D.P.H. Hasselman, Thermal stress resistance parameters for brittle refractory ceramics: a compendium, Am. Ceram. Soc. Bull. 49 (12) (1970) 1033–1037.
[10] P.S. Turner, Thermal-expansion stresses in reinforced plastics, J. Res. Natl. Bur. Stand. 37 (4) (1946) 239–250.
[11] N. Tamari, I. Kondoh, T. Tanaka, H. Katsuki, Mechanical properties of alumina−mullite whisker composites, J. Ceram. Soc. Japan 101 (6) (1993) 721–724.
[12] British Standard Testing of Engineering Ceramics, BS 7134 Section 1.2, 1989.
[13] ASTM C1161–90, Standard test method for flexural strength of advanced ceramics at ambient temperature, Annual Book of ASTM Standards 15.01 (1991) 327–333.
[14] ASTM D790M-86, Standard test methods for flexural properties of

unreinforced and reinforced plastics and electrical insulating materials, Annual Book of ASTM Standards 08.01 (1988) 290–298.
[15] D.R. Larson, J.A. Coppola, D.P.H. Hasselman, R.C. Bradt, Fracture toughness and spalling behaviour of high-Al_2O_3 refractories, J. Am. Ceram. Soc. 57 (10) (1974) 417–421.
[16] W.F. Brown, J.E. Srawley, Plane strain crack toughness testing of high strength metallic materials, ASTM Spec. Tech. Publ., No 410 (1967) 1–23.
[17] S.J. Burnett, Properties of refractory materials, UKAEA Research Group Report, Harwell, 1969.
[18] J.F. Shackelford, W. Alexander, J.S. Park, CRC Materials Science and Engineering Handbook, CRC Press, Boca Raton, FL, 1994.